Jül-Conf-45 D2-5

I C A N S - V

MEETING OF THE INTERNATIONAL COLLABORATION ON

ADVANCED NEUTRON SOURCES

June 22-26, 1981

Measurement of Time Structure and Thermal Neutron Spectra for Various Target-Moderator-Reflector Configurations of an Intensity-Modulated Spallation Neutron Source

G.S. Bauer*, H.M. Conrad*, H. Spitzer*, K. Friedrich** and G. Milleret***

* Inst. f. Festkörperforschung der KFA Jülich GmbH

** Physikalisch-Technische Bundesanstalt, Braunschweig

*** Laboratoire National SATURNE, Saclay, France

Abstract

Lead and uranium spallation targets have been bombarded with proton pulses of about 0.14×10^{-3} s duration at a repetition rate of 100 s^{-1} and an energy of 1.1 GeV. The spectra of neutrons thermalized in compact or grooved polyethylene moderators with lead or beryllium reflectors have been investigated. Also, the dwell-times of the neutrons in the moderator were measured. The grooved moderator gives a softer spectrum than the compact one. The same holds for the use of a beryllium reflector as compared to the lead reflector. The dwell-times of the neutrons in the polyethylene moderator depend on both the neutron energy and the target-moderator-reflector arrangement. Lead was found superior to beryllium as reflector material for an intensity modulated spallation neutron source, because it results in a better time structure without loss in peak intensity of the neutron pulses.

1. Introduction

Mainly three questions were to be investigated by measuring the thermal neutron leakage from moderators in different target-reflector configurations. From the thermal spectrum we wanted to determine the effective moderator temperature (Maxwell temperature) in order to deduce a relation of moderator geometry as well as target/reflector combinations to the hardness of the spectrum. Next we wanted to study the energy dependence of the decay times of the thermal neutron field in the moderator and finally the influence of different target/reflector combinations on these decay times. These latter questions are important in the optimization of the configurations with respect to physical and technical parameters. Physically one wants to obtain a short residence time of thermalized neutrons in the moderator to avoid long tails of the monochromatic neutron pulses extracted from the designed spallation source. Technically one is interested in an easy-to-build and inexpensive target-moderator-reflector combination.

The measurements were performed at the French proton synchrotron SATURNE which could deliver the desired 1.1 GeV protons and were a time structure of the proton pulses similar to the one proposed for the German SNQ-project could be obtained.

2. Experimental details

2.1 The experimental set-up

To simulate the conditions of the projected spallation source the beam was extracted from the ring accelerator with 100 s^{-1}. The pulse duration was about 140 µs (FWHM). The target and detector set-up was very similar to that used in previous experiments at CERN /1/ and therefore will be described only briefly (see also Fig. 1).

The pulsed proton beam with an average of 2.9×10^9 p/s hit the lead or uranium targets surrounded by moderators and reflectors as described in section 2.2.

The neutrons slowed down in the polyethylene moderator (used instead of water for experimental reasons) were extracted at 90° relative to the proton beam. For the spectra measurements the detector was placed in a straight-through position to perform an energy selection of the neutrons by time-of-flight. The measurement of the pulse structure was accomplished by placing a graphite crystal into the beam path, which deflected certain well-defined neutron energies through an angle of 90° and thus enabled the measurement of their intensity as a function of time (see Fig. 1).

An [002]-oriented pyrolytic graphite crystal was placed in reflection configuration in the thermal neutron beam, thus forming a selective velocity filter. If stored according to their time-of-arrival at the detector, neutrons of different velocities are thereby distinguished by assignment to different orders of the crystal reflections, except for an overlap caused by the "tails" of the time distribution due to an insufficiently long flight path.

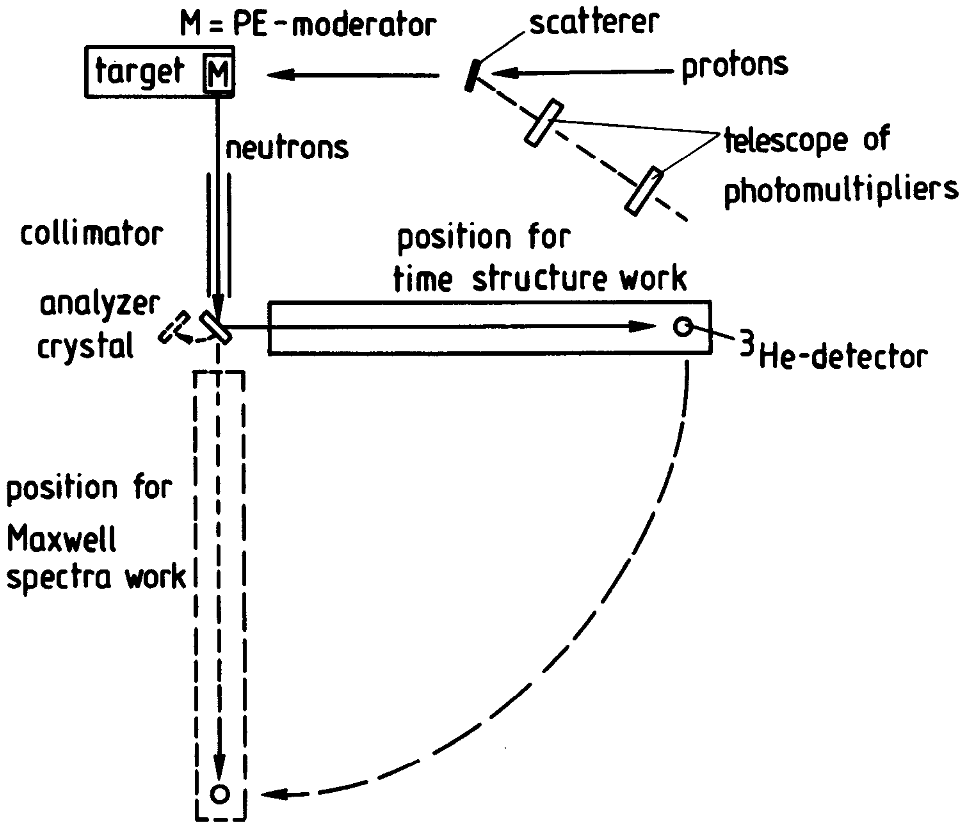

Fig. 1: Schematic (top) view of the experimental set-up

A CANBERRA multichannel analyzer MODEL 8603, into which the data from a time-of-flight interface were fed, was used for data acquisition. The neutron detector (^{3}He and BF_3) counts and the photomultiplier counts representing the primary proton distribution were stored in 2048 time channels of 4 μs width simultaneously. In some cases the counts recorded with a low-efficiency fission chamber placed in the grooves of the moderator were also stored. These latter data represent the average dwell-time of neutrons in the moderator and were necessary for defining the time-zero and the time-resolution for the Maxwell- spectra work. The time correlation between proton pulse, fast neutron background in the detector and neutron flux in the moderator is shown in Fig. 2.

The multi-channel analyzer was triggered by the 100-Hz-machine-signal from the accelerator. For the time structure work (crystal reflection data) the experimental resolution function is represented by the shape of the primary proton pulse (photomultiplier data). Fig. 3 compares its shape to the shape of the pulse for neutrons of 14.4 meV of energy (004-reflection).

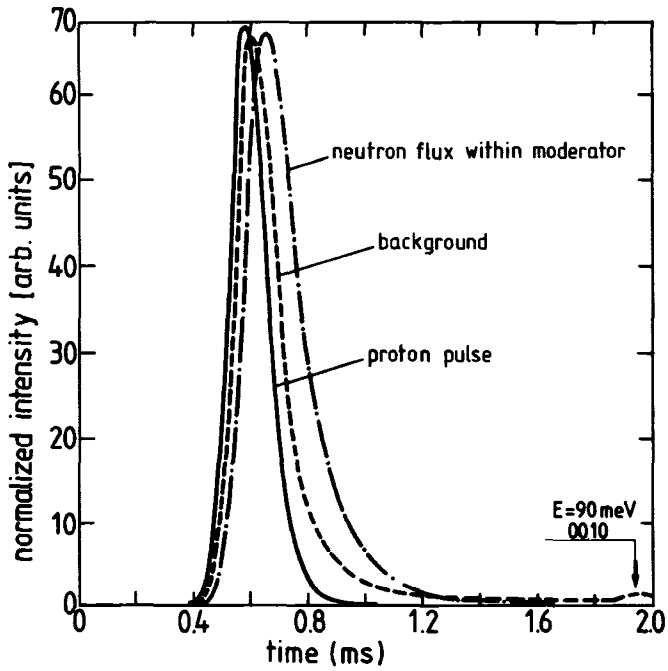

Fig. 2: Sequence and shape (on the actual time scale) of proton pulse, fast neutron background in the counter and neutron flux measured in the moderator grooves

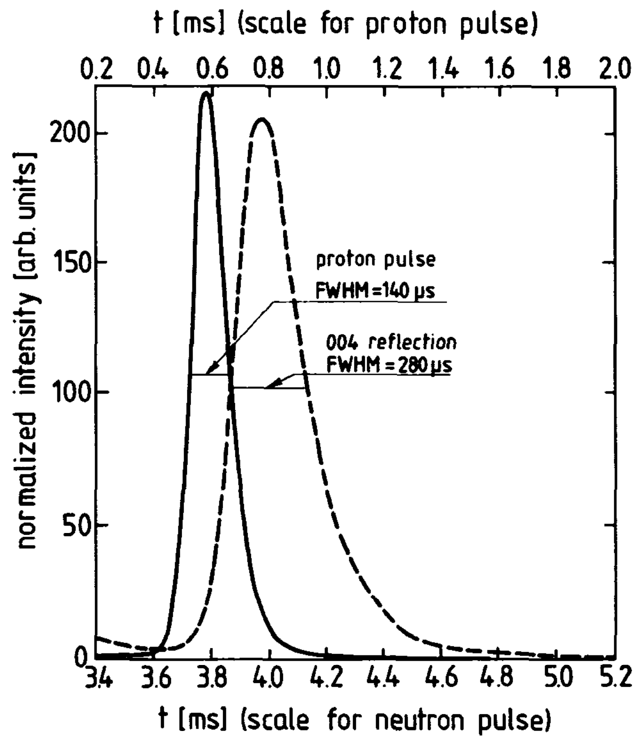

Fig. 3. Comparison of the shapes of the proton signal (employed as the resolution function) and one of the crystal analyzer reflections. (Note the shift of time scales!)

2.2 The various target-moderator-reflector configurations

The standard set-up of target-moderator-reflector combinations is shown in Fig. 4. The graphite below the target was used to simulate to some extent the D_2O-tank of a hybrid moderator configuration. It remained unchanged in the course of the experiments, whereas different combinations of the fast moderator, (simulated by compact or grooved polyethylene), and target as well as reflector materials were used (see Table 1).

	target	reflector
fast moderator (grooved)	Pb Pb U U	Pb Be Be Pb
fast moderator (compact, "flat")	Pb	Pb

Table 1: Target-moderator-reflector configurations investigated

Only one configuration with a compact fast moderator was tested for comparison, as it was known from earlier experiments that the grooved moderator gives an intensity gain of about a factor of 2 /4/. (The grooves have been worked into the moderator face pointing towards the neutron extraction channel.)

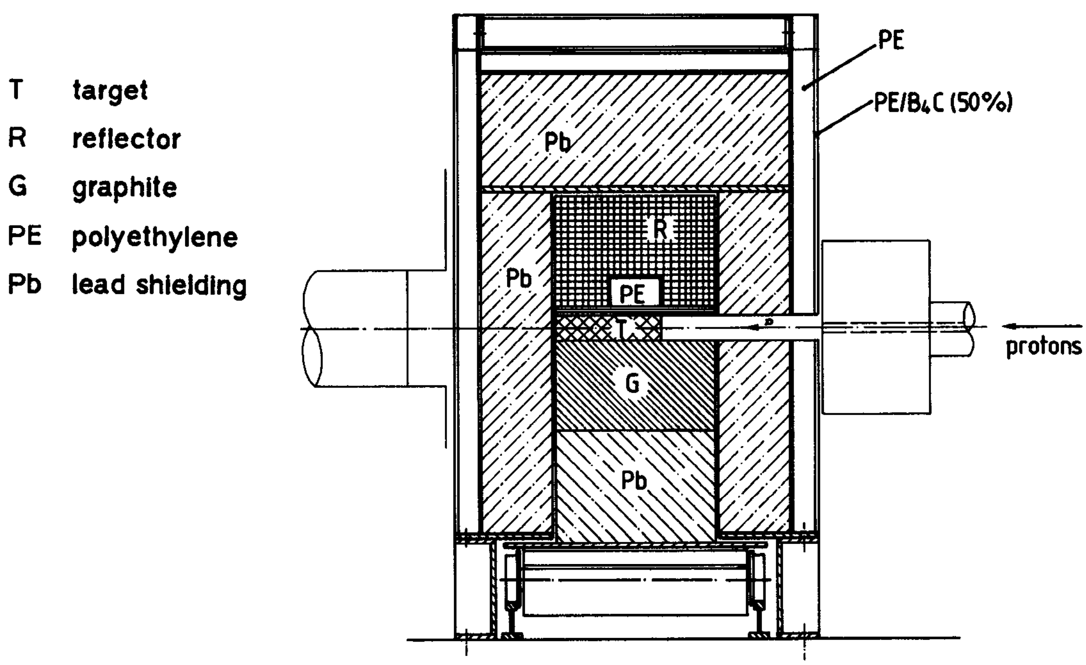

Fig. 4: Target-moderator-reflector arrangement

3. Experimental results and data evalution

3.1 Thermal neutron spectra

In Fig. 5 a typical example of the distribution of flight-times of the neutrons emerging from the fast moderator is shown, as measured in a distance of about 5.5 metres from the moderator. (This is little less than the distance of the moderator from the outer surface of the shielding of the projected spallation source.) In addition to the Maxwellian spectrum, a contribution of fast and epithermal neutrons is present at short flight times.

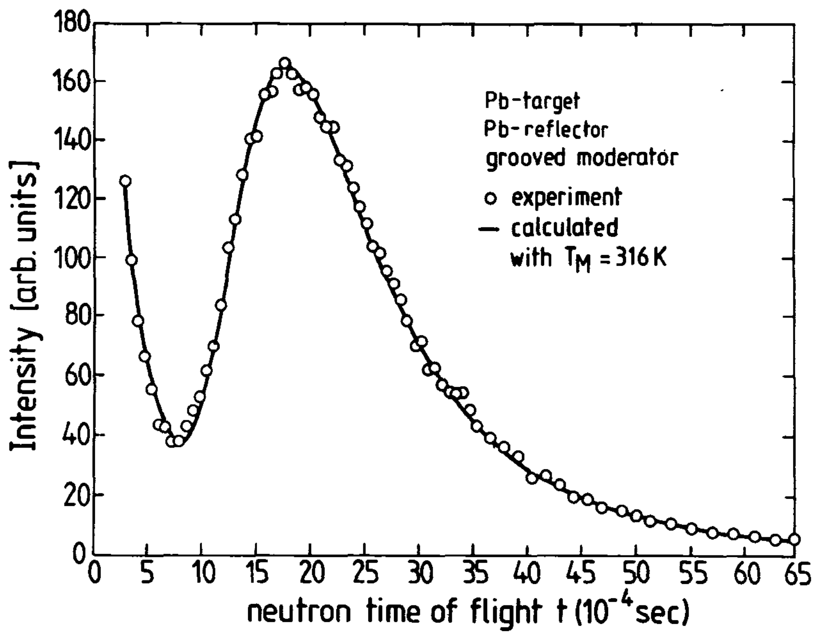

Fig. 5: Time-of-flight spectrum of neutrons emerging from the grooved polyethylene moderator (Pb target and Pb reflector). Open circles are the experimental data points (summed up over 16 4-μs-time-channels) and the solid line is a fit as described in the text.

As can be seen from Fig. 5 , the measured data could be fairly well described by a Maxwell distribution superimposed on a power-law for the fast background ($E^{-1+\alpha}$). In order to obtain the characteristic parameter of the Maxwell spectrum, i.e. the Maxwell temperature, the assumed functional expression was transformed into the time scale of the experimental data and fitted to these data using a least-squares-procedure /2/.

Two corrections have been applied to the mathematical expression to adequately describe the experimental situation. These corrections were:

a) accounting for the energy dependence of the counter efficiency, and

b) accounting for the finite width of the thermal neutron peak in the moderator (resolution correction).

The second correction was applied by convoluting the measured thermal neutron distribution in the moderator (determined experimentally with a small fission chamber placed in the moderator grooves) with the following expression (t = time of flight, with t = 0 defined at the maximum of the neutron flux pulse in the moderator; compare also Fig. 2):

$$I(t) = P_1 \cdot [(\frac{t_M}{t})^4 \cdot \exp(-\frac{t_M^2}{t^2}) + \frac{P_2 \cdot t^{-2\alpha}}{1 + (\frac{\sqrt{5}t}{t_M})^{14}}]$$

The convolution was then fitted to the experimental data by varying the parameters P_1, P_2, α and t_M, t_M being the "Maxwell-time", which can be easily transformed to give the Maxwell temperature T_M. (The denomimator in the second term of the above equation acts as a step function truncating the $E^{-(1-\alpha)}$-dependence at about $E = 5 \cdot k_B T_M$.) The velocity dependence of the counter efficiency (1/v) is already contained in the above expression. A list of the results for the Maxwell temperatures obtained by this evaluation procedure is given in Table 2. (The more or less unimportant scale factors P_1 and P_2 were omitted.)

	target	reflector	T_M[K]	α
grooved PE-moderator	Pb	Pb	316 ± 4	o.68 ± 0.10
	Pb	Be	284 ± 5	0.36 ± 0.14
	U	Be	293 ± 5	0.24 ± 0.12
	U	Pb	322 ± 3	0.48 ± 0.10
"flat" PE-moderator	Pb	Pb	355 ± 6	0.54 ± 0.07

Table 2: Maxwell temperatures of different target-moderator-reflector configurations. Little relevance should be attributed to the values of α (see discussion).

One remark should be added concerning the resolution function. In fact, the dwell time of the thermal neutron field in the moderator is a function of neutron energy. This is physically obvious, since faster neutrons leave the moderator volume faster and has also been found in the time structure measurements performed at CERN /1/ and in this work (see next section). For this reason, strictly speaking, an energy-dependent resolution function should be used. In our case, due to the long proton pulses the resolution is dominated by the width of the "prompt" thermal neutron pulse in the moderator, which is of the order of the dwell times found in the following section. Therefore we used one single resolution function for all energies (flight times).

3.2 Time structure of crystal reflections

In order to obtain the dwell times of the neutrons of different energies in a fairly wide energy range it is necessary to evaluate as many orders of reflections as possible. Unfortunately the higher orders are difficult to measure for mainly three reasons. Firstly, they decrease in intensity at high energies due to the shape of the Maxwell spectrum, secondly, they become less and less separable because of the t^{-3}-dependence of time-of-flight spectra and thirdly, the highest orders are superimposed on a steep background of fast neutrons because of the poor shielding in these experiments (see Fig. 6).

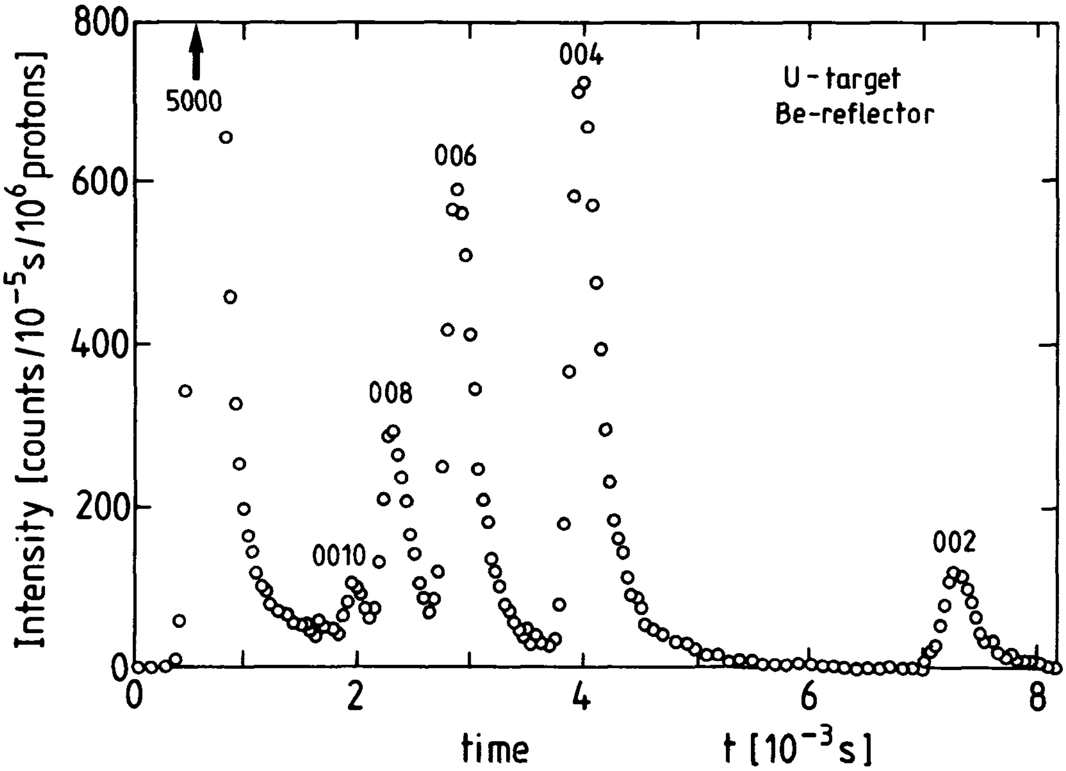

Fig. 6: Graphite analyzer crystal reflections and fast neutron background (peak intensity of background: 5000.)

This background was, of course, subtracted in our evaluation procedure (see Fig. 7), but the statistical errors quickly become considerable for higher order reflections due to the difference of nearly equal numbers. The background was measured with the crystal analyzer rotated out of reflection position and subtracted from the crystal data normalized to the number of protons recorded.

For the analysis of the dwell times the complete scan was partitioned into five sections containing one observable reflection each, by chosing six channel numbers to define five evaluation intervals. For reasons of computation time each reflection was treated separately after subtraction of

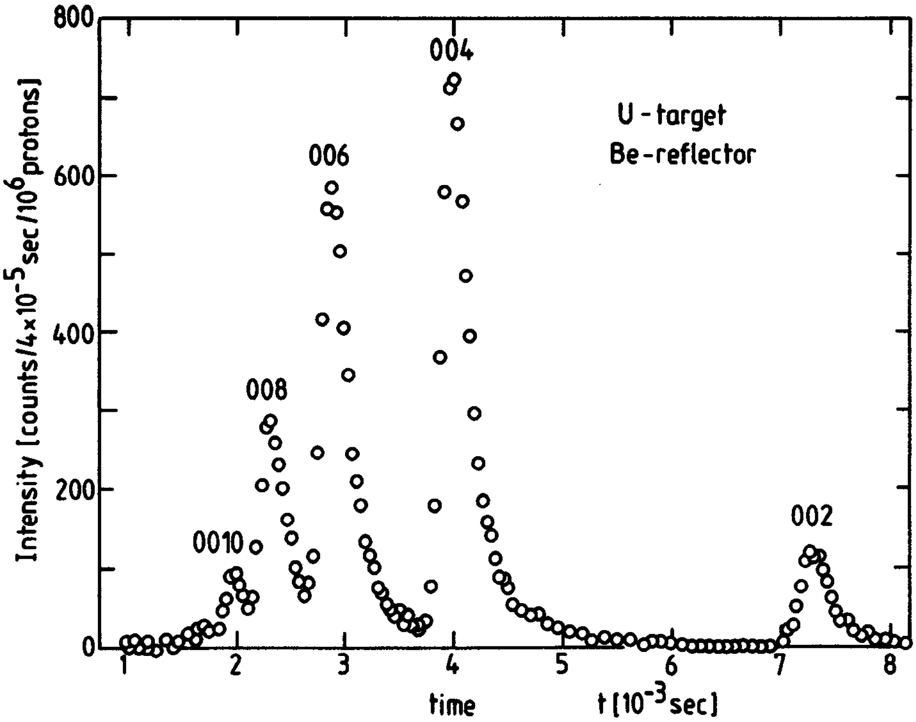

Fig. 7: Normalized crystal analyzer scan (background subtracted) revealing the finite neutron dwell time in the moderator (saw-tooth characteristic of the crystal reflections).

the overlap from higher order reflections obtained by extrapolation of the exponential decay. The detailed procedure was as follows. Starting with the highest observable reflection order ([0010] in this experiment) an exponential decay law of the form

$$f(t) = P \cdot \exp[-(t-t_o)/\tau] \quad \text{for } t \geq t_o$$
$$f(t) = 0 \quad \text{for } t < t_o \qquad (1)$$

was assumed and weighted according to the normalized distribution p(t) of the primary proton intensity. This resulted in the expression

$$I(t) = P \cdot \int_{t_a}^{t} p(t')\exp[-(t-t'+t_a)/\tau]dt' \qquad (2)$$

which was fitted to the experimental data by varying the parameters P, t_a and the dwell-time τ /3/. (The parameter t_a defines the zero-point within the different selected reflection intervals, i.e. the lower limit of the proton distribution function p(t). The boundary condition of equ. 1 was applied to equ. 2 accordingly.)

It should be mentioned that in the case of the lead reflector we found it sufficient to use only one time-constant to fit the data within the resolution of this experiment (see also section 4.2). On the other hand the peaks obtained with the beryllium reflector exhibited more pronounced tails for longer times than with the lead reflector, as can be seen in Fig. 8. Therefore we applied eq. (2) with two exponentials and two decay constants τ_1^{-1} and τ_2^{-1} respectively. Some representative fits are shown in Fig. 9.

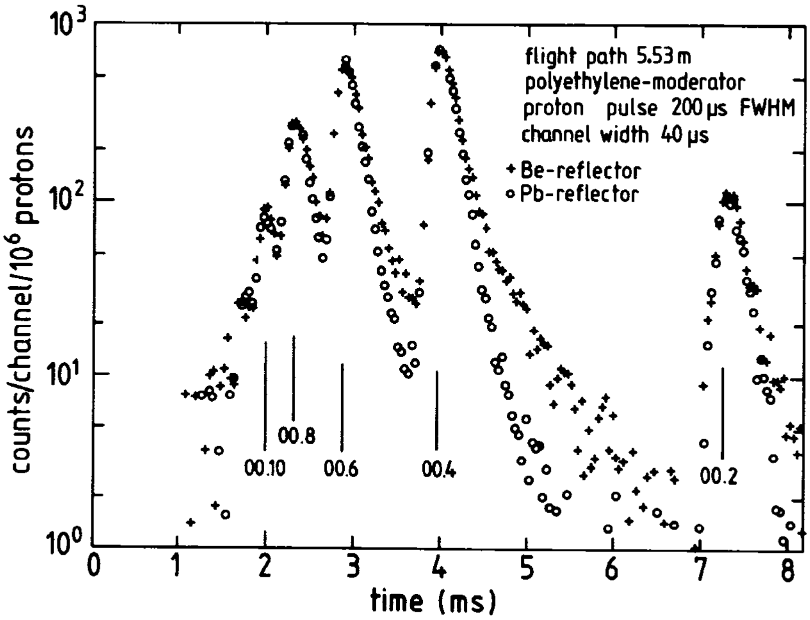

Fig. 8: Comparison of analyzer crystal reflections for two different reflector materials. Clearly, the Be-reflector exhibits wider tails.

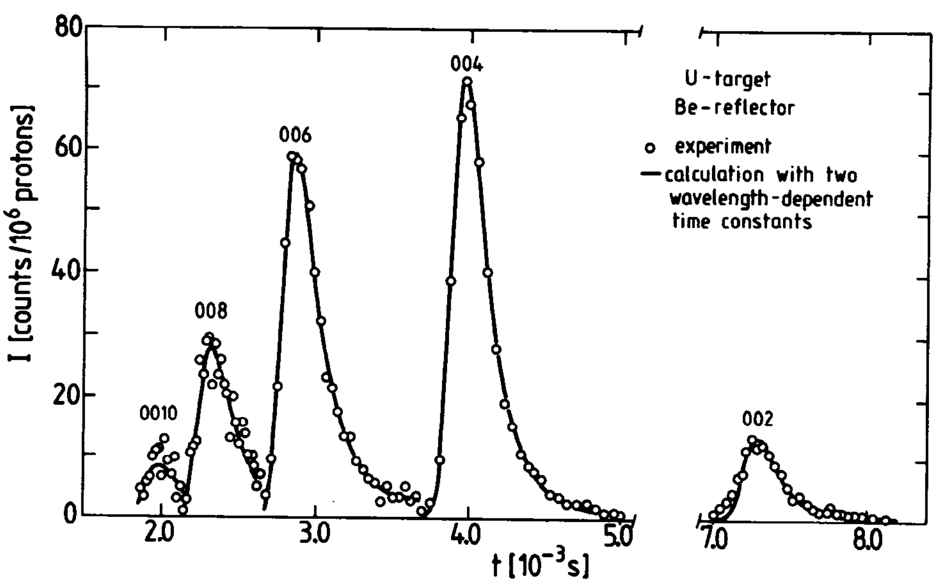

Fig. 9: Example of the numerical fits for a set of analyzer crystal reflections. The solid line is the convolution of the thermal neutron distribution (measured in the moderator) with two exponentials as described in the text.

A compilation of numerical results for the different target - moderator - reflector configurations is given in Table 3.

configuration		dwell times τ [10^{-6}s] and scale factors P [relative units]				
		order of crystal reflection				
(target -reflector -moderator)		002 (3.64 meV)	004 (14.4 meV)	006 (32.8 meV)	008 (57.8 meV)	0010 (90.3 meV)
Pb-Pb-"flat"	τ	184 ± 10	188 ± 4	169 ± 4	125 ± 5	(300)
	P	4.3 ± 0.3	29.6 ± 0.7	28.5 ± 0.7	16.1 ± 0.6	(4.2)
Pb-Pb -grooved	τ	152 ± 5	168 ± 3	178 ± 3	167 ± 8	278 ± 58
	P	15.2 ± 0.6	76.7 ± 1.5	56.1 ± 0.9	24.6 ± 0.9	8.4 ± 0.7
Pb-Be -grooved	τ_1	118 ± 28	140 ± 15	134 ± 55	(165 ± 383)	22 ± 17
	P_1	10.5 ± 1.3	55.1 ± 3.7	44.1 ± 3.8	(21. ± 100.)	(3.9 ± 11.4)
	τ_2	469 ± 258	482 ± 125	505 ± 64	(437 ± 10^4)	(249 ± 316)
	P_2	1.7 ± 1.6	9. ± 4.5	7.1 ± 4.7	(0.5 ± 96.)	(5.6 ± 5.9)
U-Pb -grooved	τ	132 ± 5	128 ± 3	139 ± 3	115 ± 4	198 ± 35
	P	26.6 ± 1.2	168. ± 5.	125. ± 3.	63.6 ± 2.1	13.4 ± 1.
U-Be -grooved	τ_1	102 ± 35	151 ± 9	153 ± 10	(151 ± 600)	(115 ± 600)
	P_1	25.7 ± 2.7	141. ± 5.	115. ± 3.	(55.8 ± 10^3)	(19. ± 120)
	τ_2	397 ± 240	577 ± 400	(9771 ± 10^5)	(239 ± 10^3)	($3 \cdot 10^4$ ± 10^6)
	P_2	4.4 ± 3.3	3.7 ± 6.6	2.6 ± 2.	(0.4 ± 10^3)	(0.4 ± 132)

Table 3: Dwell-times of neutrons of different energies for different target-moderator-reflector-configurations. Values with low confidence level are put in parentheses.

4. Discussion

4.1 Thermal neutron spectra

Although two of the deduced Maxwell temperatures appear to be somewhat low (see Table 2), the following conclusion can be drawn. The grooved moderator exhibits a softer spectrum than the flat one. This was expected and can be understood, at least qualitatively, as from a grooved moderator slower neutrons from the interior can escape. Without the grooves these neutrons could not have reached the moderator surface due to their short mean free path in a hydrogeneous substance. Besides this spectral softening a gain in intensity of roughly a factor of 2 was observed /4/. The beryllium reflector also gave a softer spectrum, as compared to the lead reflector.

As to the exponent α (see section 3.1 and Table 2), it does not seem to constitute only a small correction (0.1 ... o.2) to an 1/E-law as expected. An obvious reason could be that there were too few data points for the fit in the relevant energy range. More likely were an experimental explanation, as the background was not subtracted for technical reasons. The background clearly does not obey an 1/E law and therefore may falsify the α-values. An interference of these most likely unphysical α's with the result for the Maxwell temperatures can be excluded because of the small overlap of these contributions (see Fig. 5).

4.2 Time structure of crystal reflections

The energy, respectively velocity dependence of the thermal neutron field in a finite moderator can certainly not be described mathematically by a few parameters only. The spatial flux distribution ought to be represented properly by a Fourier series, each of its components revealing a different dwell time. Although one or two time-constants will normally be dominating it might appear fairly arbitrary to describe the situation with only one or two time constants for each velocity band, i.e. order of reflection of the analyzer crystal. On the other hand, in view of the resolution of this experiment, it seemed not reasonable to use more parameters.

For an easier interpretation of the results some additional figures have been calcualted from the fit parameters. These were:

a) the integrated intensity $I = P \cdot \tau$, resp. $I = P_1\tau_1 + P_2\tau_2$ in the cases of the Be reflectors,

b) the ratio of integrated intensity to peak maximum, i.e. $I/P = P\tau/P$, which is the "unfolded width" τ of the reflection. In the case of a superposition of exponentials this value is an "effective" width τ_{eff} $\tau_{eff} = (P_1\tau_1 + P_2\tau_2)/(P_1 + P_2)$, and

c) the standard deviation S (= square root of the normalized second moment) $S = \sqrt{\sigma^2}$, with $\sigma^2 = 2P\tau^3/I = 2\tau^2$ and $\sigma^2 = 2(P_1\tau_1^3 + P_2\tau_2^3)/(P_1\tau_1 + P_2\tau_2)$ respectively.

A compilation of these results is given in Table 4.

configuration (target-reflector -moderator)	integr. intensity I I_{max} (= P, resp. P_1+P_2) $I/I_{max} = \tau_{eff}$ standard deviation S	order of crystal reflection				
		002 3.64 meV	004 14.4 meV	006 32.8 meV	008 57.8 meV	0010 90.3 meV
Pb-Pb-"flat"	I [relative units]	0.78	5.6	4.8	2.0	1.3
	I_{max} [relative units]	4.3	29.6	28.5	16.1	4.2
	τ_{eff} [10^{-3}s]	0.184	0.188	0.169	0.125	(0.300)
	S [10^{-3}s]	0.260	0.266	0.239	0.177	(0.424)
Pb-Pb-grooved	I	2.3	13.	10.	4.1	2.3
	I_{max}	15.2	76.7	56.1	24.6	8.4
	τ_{eff}	0.152	0.168	0.178	0.167	(0.278)
	S	0.215	0.236	0.252	0.236	(0.393)
Pb-Be-grooved	I	2.	12.	9.5	3.7	1.5
	I_{max}	12.2	64.1	51.2	21.5	9.5
	τ_{eff}	0.166	0.188	0.185	0.171	0.156
	S	0.433	0.439	0.463	0.271	(0.343)
U-Pb-grooved	I	3.5	22.	17.	7.3	2.7
	I_{max}	26.6	168.	125.	63.6	13.4
	τ_{eff}	0.132	0.128	0.139	0.115	(0.198)
	S	0.187	0.181	0.197	0.162	(0.281)
U-Be-grooved	I	4.4	23.	(43.)	8.5	(14.)
	I_{max}	30.1	145.	118.	56.2	19.3
	τ_{eff}	0.145	0.162	(0.366)	0.152	(0.750)
	S	0.373	0.320	(10.6)	0.216	(42.3)

Table 4: Integrated intensities, effective widths and standard deviations of the crystal reflections for different target-reflector-moderator configurations. Numbers of small confidence levels are put in parentheses.

In the cases of the lead reflector the effective dwell-times τ_{eff} are identical to the τ-values of Table 3. For the Be reflector configurations an effective broadening is observed, which was already apparent from the raw data (see Fig. 8).

A more sensitive indicator of the "broadening" is the standard deviation S of the intensity distribution within the reflections since it weighs the "tails" more heavily. The S-values for the beryllium reflector are significantly larger than those of the lead reflector.

As all results have been normalized to 10^6 primary protons, a quantitative comparison with respect to intensities can be made for the different configurations. The gain of roughly a factor of two found for the grooved moderator as compared to a compact ("flat") one by measuring the neutron leakage flux /4/ was established (compare line 1 and 5 of Table 4). Using uranium instead of lead as target material yields an additional gain of a factor of two.

For the efficient application of mechanical choppers as "tail-cutters" it is important to obtain pulse structures with large peak intensities. From the values of I_{max} in Table 4 one can see that the lead reflector fulfills this condition better than the beryllium one.

Summarizing we can conclude:

1) For an intensity modulated neutron source, no decoupler is used and the time structure is to be taken advantage of for the separation of higher order reflections from the monochromator, Pb is to be preferred as a reflector material as compared to Be because of its better time structure and comparable peak flux.

2) The dwell time of 200 µs, which has been used to estimate the peak-to-average flux ratio /5/ for the intensity modulated source is too long. This means, that it underestimates the peak flux of the source.

References

/1/ G.S. Bauer, J.P. Delahaye, H. Spitzer, A.D. Taylor and K. Werner Relative Intensities and Time Structure of Thermal Neutron Leakage from Various Moderator-Decoupler Systems for a Spallation Neutron Source; this volume

/2/ H.M. Conrad, computer program "submit.maxwell", KFA-time-sharing-system (user identification IFF 022) unpublished

/3/ H.M. Conrad, computer program "submit.zeitstrk", KFA-time-sharing-system (user identification IFF 022) unpublished

/4/ G.S. Bauer, K. Grünhagen and H. Spitzer (1980) Einige Voruntersuchungen zu wasserstoffhaltigen Moderatoren für eine Spallations-Neutronenquelle; SNQ-study report, part III A2, unpublished

/5/ G.S. Bauer, W.E. Fischer, F. Gompf, M. Küchle, W. Reichardt and H. Spitzer (1981), Thermal Neutron Leakage and Time Structure Measured for Various Target-Moderator-Reflector Configurations for a Spallation Neutron Source; this volume